1 Report No	2 Government Accession No	3 Recipient's Catalog No
NASA TM X-2823		

4 Title and Subtitle	5 Report Date
EVALUATION OF REUSABLE SURFACE INSULATION FOR SPACE SHUTTLE OVER A RANGE OF HEAT-TRANSFER RATE AND SURFACE TEMPERATURE	October 1973
	6 Performing Organization Code
7 Author(s)	8 Performing Organization Report No
Andrew J. Chapman	L-8787
	10 Work Unit No
9 Performing Organization Name and Address	502-31-50-01
NASA Langley Research Center	11 Contract or Grant No
Hampton, Va. 23665	
	13 Type of Report and Period Covered
12 Sponsoring Agency Name and Address	Technical Memorandum
National Aeronautics and Space Administration	14 Sponsoring Agency Code
Washington, D.C. 20546	

15 Supplementary Notes

16 Abstract

Reusable surface insulation materials, which have been developed as heat shields for the space shuttle, have been tested over a range of conditions including heat-transfer rates between 160 and 620 kW/m^2. The lowest of these heating rates was in a range predicted for the space shuttle during reentry, and the highest was more than twice the predicted entry heating on shuttle areas where reusable surface insulation would be used. Individual specimens were tested repeatedly at increasingly severe conditions to determine the maximum heating rate and temperature capability.

A silica-base material experienced only minimal degradation during repeated tests which included conditions twice as severe as predicted shuttle entry and withstood cumulative exposures three times longer than the best mullite material. Mullite-base materials cracked and experienced incipient melting at conditions within the range predicted for shuttle entry. Neither silica nor mullite materials consistently survived the test series with unbroken waterproof surfaces. Surface temperatures for a silica and a mullite material followed a trend expected for noncatalytic surfaces, whereas surface temperatures for a second mullite material appeared to follow a trend expected for a catalytic surface.

17. Key Words (Suggested by Author(s))	18 Distribution Statement
Heat shield Surface insulation Space shuttle	Unclassified – Unlimited

19. Security Classif. (of this report)	20. Security Classif. (of this page)	21. No. of Pages	22. Price*
Unclassified	Unclassified	26	Domestic, $3.00 Foreign, $5.50

*For sale by the National Technical Information Service, Springfield, Virginia 22151

EVALUATION OF REUSABLE SURFACE INSULATION FOR SPACE SHUTTLE OVER A RANGE OF HEAT-TRANSFER RATE AND SURFACE TEMPERATURE

By Andrew J. Chapman
Langley Research Center

SUMMARY

Reusable surface insulation materials, which have been developed as heat shields for the space shuttle, have been tested over a range of conditions including heat-transfer rates between 160 and 620 kW/m^2. The lowest of these heating rates was in a range predicted for the space shuttle during reentry, and the highest was more than twice the predicted entry heating on shuttle areas where reusable surface insulation would be used. Individual specimens were tested repeatedly at increasingly severe conditions to determine the maximum heating rate and temperature capability.

A silica-base material experienced only minimal degradation during repeated tests which included conditions twice as severe as predicted shuttle entry and withstood cumulative exposures three times longer than the best mullite material. Mullite-base materials cracked and experienced incipient melting at conditions within the range predicted for shuttle entry. Neither silica nor mullite materials consistently survived the test series with unbroken waterproof surfaces. Surface temperatures for a silica and a mullite material followed a trend expected for noncatalytic surfaces, whereas surface temperatures for a second mullite material appeared to follow a trend expected for a catalytic surface.

INTRODUCTION

Reusable surface insulation materials, which are formed by rigidizing low-density ceramic fibers and applying a dense, high-emittance coating, are being developed as heat shields for the space shuttle orbiter. Requirements for these materials include reusability for as many as 100 missions, an operational life as long as 10 years, and a capability to exceed design temperatures without catastrophic failure. The ceramic materials are potentially reusable because they are chemically inert at the reentry temperatures predicted for much of the orbiter surface. Recent development and design efforts (ref. 1)

focus on applying the materials in such a way that they will withstand the rigorous mechanical and thermal environments encountered during all phases of shuttle operation.

Three materials, developed by three separate contractors, were investigated. One material was composed primarily of silica (SiO_2), and two other materials were composed primarily of mullite ($3Al_2O_3 \cdot 2SiO_2$). The materials were tested over a range of heating rate, enthalpy, and pressure in an arc-heated supersonic wind tunnel. The lowest heating rates were in a range predicted for peak heating to certain areas on the space shuttle orbiter wing lower surface during a nominal entry trajectory. The highest heating rate was about twice the highest predicted shuttle heating rate for these areas. The objectives of these tests were to evaluate the maximum heating rate and temperature capability of these materials and to determine surface temperature as a function of heat-transfer rate.

Physical quantities in this paper are given in the International System of Units (SI), but they were measured in U.S. Customary Units. Factors relating the two systems are given in reference 2.

MATERIALS AND TEST SPECIMENS

The reusable surface insulation (RSI) materials tested in this study are presented in table 1 in groups according to the manufacturer who developed them. The composition is given for the fibers, the rigidizing binder, and the coating. The densities shown are values furnished by the manufacturer.

The configurations of the specimens tested during this study are shown in figure 1. The 9-cm-square specimens that were coated on the top surface and four sides were furnished in that form by the manufacturers. Other 9-cm-square specimens and the 13-cm-square specimens were cut to size from 30-cm-square tiles and were coated on only the top surface.

All specimens were instrumented with five chromel-alumel thermocouples attached to 0.8-mm-thick copper disks bonded directly to the back surface. One thermocouple was mounted at the center of the specimen and four other thermocouples were attached at distances of 1.8 or 2.5 cm (for the 9- and 13-cm specimens, respectively) from the center along a longitudinal and lateral center line of the specimen. Certain specimens were also instrumented with thermocouples at the center of the top surface. These thermocouples were platinum/platinum-13% rhodium and were installed by the manufacturer during the specimen fabrication. The thermocouple bead was located approximately at the midthickness of the coating and the thermocouple wires ran approximately 7 mm parallel to the surface coating.

TEST PROCEDURES

For testing, the specimens were attached to a water-cooled copper holder, shown in figure 2, and exposed to heating in an arc-heated supersonic wind tunnel. As shown in figure 2, the specimens were mounted on the side of the wedge-shape holder with the top surface of the specimen flush with the forward surface of the holder. The back surface and forward sides of the specimen were insulated from the holder. The test facility, apparatus D of the Langley entry structures facility, is described in reference 3. In the present investigation, models were tested at nine conditions which are described in table 2.

Calibration Tests

Prior to the materials tests, a series of heat-transfer calibration tests was made at each of the nine test conditions. A thin-wall calorimeter, installed in the holder, was used to measure heat-transfer-rate distribution. The thin-wall heat-transfer measurements were referenced to measurements made by using a hemispherical probe instrumented with a continuous-reading heat-transfer gage, and heating conditions in the materials tests were determined from the hemispherical probe. Heat-transfer-rate distributions over the calorimeter at each test condition are shown in figure 3. During each calibration test, stagnation pressure was measured on a pitot probe.

Test and Predicted Space Shuttle Heating Rates

Predicted entry heating-rate histories for two areas on the space shuttle orbiter wing lower surface are shown in figure 4. These conditions were developed by the NASA Lyndon B. Johnson Space Center as a baseline for thermal protection system studies. Area 2 is just aft of the wing leading edge and area 1 is somewhat farther aft. Perturbed heating conditions on area 2 (designated area 2P) were the highest heat-transfer rates considered for areas on the shuttle where RSI would be used. Test condition 1 compares with heating for area 2, and test condition 2 is somewhat higher than peak heating for area 2P. The test heat-transfer rates are for the center of the specimen ($x/L = 0.5$ and $y = 0$ in fig. 3). However, these square-heat-pulse test conditions, which produce abrupt thermal shock on insertion into and removal from the test stream, are more severe than the shuttle entry trajectories which produce the gradual heating and cooling shown by the heating-rate histories. Test conditions 3 to 9 were more severe than any normal shuttle entry heating predicted for areas aft of the nose cap and leading edges.

Specimen Tests

The 13-cm-square specimens were tested only at the lowest heating condition. The 9-cm-square specimens from each material were tested at the progressively severe test

conditions shown in table 2 up to condition 9 or until degradation such as extensive melting and cracking, which would destroy the integrity of the specimen, was observed. Some materials could not withstand the more severe conditions, and for these materials a new specimen was tested at less severe conditions.

At the beginning of each test, the arc tunnel was started and stable operating conditions were established. A reference cold-wall heating rate was measured on the hemispherical probe and the stagnation pressure was measured on the pitot probe. The specimen was inserted into the test stream. The specimen was removed from the stream when the back surface temperature had increased 167 K above the pretest value. After withdrawal from the test stream, specimen temperatures were recorded until maximum values were reached at each point of measurement.

Normally, the arc-tunnel test section remained closed and at reduced pressure between tests, to conserve the time and power required to establish low pressure in the test section. The general condition of the specimen was observed through the test-section window. Specimens were available for close examination only during prolonged pauses and at the conclusion of a test series. During close examination, the condition of the specimen was observed and a pattern of water drops was applied over the surface to determine if the coating remained waterproof.

During the tests, surface temperature of the specimens was measured by a radiation pyrometer which senses radiation in a range of 2.0 to 2.6 μm. In reducing the radiometer output data to temperatures, the materials were assumed to have an emittance of 0.7.

RESULTS AND DISCUSSION

The test results for each material and specimen are summarized in table 3. The results of the repeated tests of each specimen are shown in figures 5 and 6. The exposure periods for each specimen are plotted at the heat-transfer rate for the center of the specimen ($x/L = 0.5$ and $y = 0$ in fig. 3) and are plotted in sequence so that the time indicated at the end of the last exposure period is the cumulative exposure for that specimen. The photographs show the condition of each specimen at the conclusion of a test series.

Tests at Nominal Shuttle Entry Conditions

The results of testing three materials at test condition 1, nominal shutter entry condition, are shown in figure 5. The heating rate of this test condition corresponds closely to the shuttle peak area 2 heating shown in figure 4, although the tests were more severe than shuttle entry because of the abrupt heat-up and cool-down. As noted previously, the 13-cm-square specimens were not coated on the sides and did not have a surface thermocouple.

Silica specimen S-1 accumulated 14 216 seconds exposure during six consecutive tests. After this test series, the coating did not appear to be degraded; however, there was a microscopic crack in the surface through which water penetrated. Mullite specimen MA II-1 accumulated only 2036 seconds exposure during three consecutive tests, after which the forward area of the coating was discolored, covered with small blisters, and penetrated by a large crack. Mullite specimen MB I-2 accumulated only 1049 seconds exposure during two tests after which the entire surface was degraded and pitted and the forward edge was glazed as a result of melting.

At test condition 1, the silica material survived with minimal degradation, whereas the mullite coatings not only cracked but showed evidence of incipient melting as well. Further, total exposure time for the silica was more than seven times greater than for the mullite materials.

Tests at Conditions More Severe Than Shuttle Entry

Silica material S.- Results of testing 9-cm-square specimens of material S at increasingly severe conditions are shown in figure 6(a). Specimen S-3, which was not coated on the sides and did not have a surface thermocouple, accumulated 5900 seconds exposure during nine tests. Seven of these tests represented 4470 seconds exposure at the more severe test conditions. At the end of this series of tests, the forward surface, which experienced the highest heating rates, was a somewhat lighter color than the original and was slightly warped but was otherwise undamaged. There were no visible cracks, and water did not penetrate the surface during observation.

Specimen S-4 was tested through five cycles of progressively severe test conditions through test condition 7. After this test series, the forward one-third of the surface area was slightly discolored and covered with small, granular protuberances which are believed to be evidence of incipient melting. Thin cracks through the coating extended from the surface thermocouple forward and aft. Water was not observed to penetrate through these cracks. The side coatings had no visible cracks.

Specimen S-5 was tested through three cycles beginning at test condition 5 to identify the condition where melting would begin. After the test at condition 6, the fine granular protuberances were again observed on the forward part of the top surface. These protuberances were more pronounced after testing at test condition 7, and cracks extended from the surface thermocouple. Cracks were not visible on the side. Water penetrated the coating in the vicinity of the surface thermocouple and through the cracks.

Changes, which were probably incipient melting, in the material S coating began to appear during tests at cold-wall heating rates of 530 kW/m^2 and surface temperatures of 1670 to 1700 K. However, these changes did not progress to become serious degradation,

and one specimen of material S repeatedly survived surface temperatures as high as 1850 K with only gradual and moderate changes. The only coating cracks originated where thermocouples were embedded in the coating or occurred on 13-cm specimens which experience higher thermal stresses than the smaller 9-cm specimens. Cracks were not observed in side coatings or near corners where stress concentrations are high.

Mullite material MA.- Results of testing 9-cm-square specimens of material MA III at increasingly severe conditions are shown in figure 6(b). Specimen MA III-1 was exposed for 1389 seconds during six tests. At the end of the fourth test (condition 6), the forward area of the top surface was cracked, discolored, and uneven as a result of melting. The average surface temperature at test condition 6 was 1600 K. At the end of six tests, the last at test condition 9, more than three-fourths of the top surface was rippled and uneven and the forward one-third of the surface was extensively glazed. The coating was penetrated by a wide crack on the forward half of the top surface and was also cracked along the forward side and around the forward corners. Water penetrated the cracked areas of the coating. The average surface temperature at test condition 9 was 1750 K.

Specimen MA III-2 was tested beginning at test condition 2 to establish the conditions which initiated serious degradation in this material. This specimen survived one test at test condition 2 without noticeable degradation. After two tests at condition 3, the forward one-third of the surface was somewhat lighter than the original color and had a granular texture. The coating was cracked extensively on the top surface and on the forward side extending around a forward corner. Water penetrated the coating at some large cracks and at other points where cracks were not clearly visible. Average surface temperature at test condition 3 was about 1500 K.

Since specimen MA III-2 did not survive test condition 3, specimen MA III-3 was tested through four cycles at test condition 2 to determine whether the material would survive the less severe test condition. Some granular texture was observed on the forward surface at the end of the first test. The cold-wall heating rate was 40 percent higher at the forward edge of the specimen than at the center, and during subsequent tests of specimen MA III-3 at condition 2, the radiometer was focused on the forward edge of the specimen to measure temperatures at the higher heating rate areas where degradation was occurring. These temperatures measured along the forward one-fourth of the surface were between 1480 and 1510 K as compared with 1410 K at the center. Following the fourth test cycle of specimen MA III-3, the forward one-third of the surface had the granular texture and lighter color noted previously. The top surface was cracked from the thermocouple to the forward edge and on one corner, and the cracks on the forward side extended to the corners. Water penetrated the surface at the cracks and at the surface thermocouple locations. These results show that material MA III was unable to withstand repeated testing at conditions corresponding to shuttle area 2P peak heating.

Results of testing 9-cm-square specimens of materials MA I and MA II are shown in figure 6(c). Both specimens were tested through repeated cycles ending with the most severe test condition, and both specimens were tested for a total time of approximately 1850 seconds, although the tests of MA I-1 consisted of six cycles whereas the tests of MA II-1 consisted of eight cycles of somewhat shorter duration.

The coating of specimen MA I-1 was discolored but only moderately glazed. Otherwise the coating appeared less degraded than that of the other MA materials. Specimen MA I-1 was, however, cracked on the forward side, and this crack extended to the top surface at a forward corner. Water penetrated the coating at this crack and near the surface thermocouple.

Specimen MA II-2 was not coated on the sides and did not have a thermocouple in the top surface. At the end of the test series, the top surface was extensively glazed and discolored; however, the surface was not visibly cracked and water penetration was not observed.

There was a wide variation of performance among the mullite MA materials. Material MA I, which performed best, cracked only at the high stress concentration area on the specimen forward side near a corner and experienced only incipient melting during repeated tests which included the most severe conditions. However, material MA I accumulated less than one-third the total exposure accumulated by silica material S which survived the test series with minimal degradation. Materials MA II and MA III, which were developed later than MA I, experienced cracking and incipient melting at the lower test conditions, which are within the range predicted for shuttle entry, and experienced extensive and severe melting during tests at the highest conditions. In addition, the MA materials were markedly less efficient insulators than material S. During individual tests at comparable conditions and specimen unit weights, exposure periods for a back surface temperature rise of 167 K were greater by a factor of 2 for material S than for material MA.

Mullite material MB.- Results of testing 9-cm-square specimens of material MB through increasingly severe conditions are shown in figure 6(d). Specimen MB I-3, which was coated only on the top surface, was tested seven times at seven different test conditions for a total exposure of 1372 seconds. After this testing, the entire surface was extensively glazed and pitted. Water penetrated the coating at many places.

Specimen MB II-1 which was coated on the sides as well as the top was tested five times, the final test being at test condition 7. After these tests, the forward two-thirds of the coating was glazed, pitted, and cracked. Cracks extended from the front side around the corners to the other sides and over the corners to the top surface. However, water penetrated the coating only at the surface thermocouple location.

Specimen MB II-2 was tested twice at test condition 2 before proceeding to conditions 3 and 4. After testing at condition 4, the surface was glazed and discolored; however, no cracks were visible. Water penetration of the coating was not observed.

Material MB surface temperatures were markedly higher over the range of test conditions than those of either material S or material MA. Coating degradation was extensive after relatively short tests at test condition 1, where surface temperatures were approximately 1800 K, and the coatings continued to deteriorate further through a series of tests up to test condition 7, where surface temperatures were approximately 1970 K.

RSI Surface Temperature

RSI front surface temperatures measured during each test are recorded in table I In figure 7, front surface temperatures, as measured by a radiometer, are plotted agai cold-wall heat-transfer rate. The surface temperatures were measured at the center the specimen and heat-transfer rates were determined for this location from calorimet measurements. Each data symbol in figure 7 represents one specimen, and its repetiti in a figure shows results for different tests. The experimental data are compared wit equilibrium surface temperatures which have been calculated by using a hot-wall corre tion and by assuming an emittance of 0.7. The calculated temperatures are for heat tr fer to a fully catalytic surface.

Surface temperatures for material S are shown in figure 7(a). At a heat-transfer rate of 300 kW/m^2 the measured surface temperatures were approximately equal to the calculated temperatures. At heat-transfer rates greater than 300 kW/m^2, the measure surface temperatures are lower than the calculated values and follow a consistent trenc except for data at a heating rate of 620 kW/m^2 where the temperatures measured on sp imen S-3 (circles) increased with repeated testing, possibly as a result of decreased emittance.

Surface temperatures for material MA are shown in figure 7(b). The measured t peratures fall in a band well below the computed values and are generally somewhat les than the temperatures measured on material S.

The characteristics of the specimen coatings and the test conditions suggest that difference between measured and calculated surface temperatures is primarily a result of a noncatalytic effect from the surface coatings. In reference 4, it is shown that glas materials such as the coatings on materials S and MA tend to be noncatalytic and that h transfer to a noncatalytic surface in a nonequilibrium stream is reduced as enthalpy increases. The measured temperatures agree with the calculated equilibrium tempera tures at low heating rates and stream enthalpy and are lower than the equilibrium

temperatures in the higher ranges of heating rate and enthalpy where the noncatalytic effect would be greater. A similar trend for the temperatures of glassy RSI coatings was reported in reference 5. Actual emittance values greater than the assumed value of 0.7 would also result in measured surface temperatures lower than the calculated values.

Surface temperatures over the range of heat-transfer rate for material MB are shown in figure 7(c). Surface temperatures measured on this material throughout the range of test conditions were markedly higher than the temperatures measured on either material S or material MA. The trend of these temperatures, which is considerably higher than that calculated for equilibrium surface temperatures except at the highest heating rate, suggests that the surface is catalytic and that the actual emittance is less than the assumed value of 0.7. The untested surface of material MB is originally less glassy in appearance than that of material S or material MA.

CONCLUDING REMARKS

Reusable surface insulation (RSI) materials, which have been developed as heat shields for the space shuttle, have been tested over a range of conditions including heat-transfer rates between 160 and 620 kW/m^2. The lowest of these heating rates was in a range predicted for the space shuttle during reentry, and the highest was more than twice the predicted entry heating rates on shuttle areas where RSI would be used. Individual specimens were tested repeatedly at increasingly severe conditions to determine the maximum heating rate and temperature capability.

A silicia-base material experienced only minimal degradation during repeated tests which included conditions twice as severe as predicted shuttle entry and withstood cumulative exposures three times longer than the best mullite material. Mullite-base materials typically cracked and experienced incipient melting at conditions within the range predicted for shuttle entry.

Although one silica specimen withstood the test series, unbroken waterproof surfaces were not found consistently for any of the RSI materials. Tiles coated on four sides were more prone to develop surface cracks than those coated only on the top surface. Irregularities such as thermocouples embedded in the coating tended to be sources for cracks.

Surface temperatures for a silica-base RSI and one mullite-base RSI, measured over a range of heating rates, followed a trend expected for heat transfer to a noncatalytic surface. These materials have glassy coatings which are usually noncatalytic. Surface

temperatures for a second mullite RSI followed a trend predicted for heat transfer to a catalytic surface. This material had a less glassy coating than the other RSI materials.

Langley Research Center,
National Aeronautics and Space Administration,
Hampton, Va., July 26, 1973.

REFERENCES

1. Tanzilli, Richard A.: Development of an External Ceramic Insulation for the Space Shuttle Orbiter. Contract No. NAS 1-10533, Re-entry & Environ. Syst. Div., Gen. Elec. Co., Apr. 1972. (Available as NASA CR-112038.)

2. Anon.: Metric Practice Guide. E 380-72, Amer. Soc. Testing Mater., June 1972.

3. Chapman, Andrew J.: Thermal Performance of 625-kg/m^3 Elastomeric Ablative Materials on Spherically Blunted 0.44-Radian Cones. NASA TM X-2612, 1972.

4. Pope, Rorald B.: Stagnation-Point Convective Heat Transfer in Frozen Boundary Layers. AIAA J., vol. 6, no. 4, Apr. 1968, pp. 619-626.

5. Goldstein, Howard E.; Buckley, John D.; King, Harry M.; Probst, Hubert B.; and Spiker, Ivan K.: Reusable Surface Insulation Materials Research and Development. NASA Space Shuttle Technology Conference – Dynamics and Aeroelasticity; Structures and Materials, NASA TM X-2570, 1972, pp. 373-433.

TABLE 1.- REUSABLE SURFACE INSULATION MATERIALS

Designation	Density, kg/m³	Composition		
		Fibers	Binder	Coating
S	240	Silica	Silica	Borosilicate glass, silicon carbide or silicide pigment
MA I	240	Mullite	Pyrolyzed silicone, and organometallics	Alumina, silica, lithia, and other oxides, in amorphous and crystalline phases, nickel oxide emittance pigment
MA II MA III	192	Mullite	Al_2O_3-SiO_2-B_2O_3	
MB I MB II	240	Mullite	Silica	Borosilicate glass, emittance pigments, $AlPO_4$ in multiple layers

TABLE 2.- TEST CONDITIONS

Test parameter	Test condition								
	1	2	3	4	5	6	7	8	9
Total enthalpy, MJ/kg	24	13	14	17	19	20	22	23	24
Stagnation pressure, kN/m²	6.8	5.5	5.8	6.4	6.5	6.7	7.0	7.1	7.3
Hemispherical heat-transfer parameter, kW/m²	680	320	360	480	530	550	630	680	730
Specimen cold-wall heat-transfer rate at –									
Forward location, kW/m²	295	420	510	650	680	770	910	860	920
Center location, kW/m²	130	300	360	440	490	530	610	610	620
Aft location, kW/m²	80	230	280	340	390	410	480	440	470

TABLE 3 - TEST RESULTS

(a) Material S

Specimen	Specimen size, cm	Test cycle	Test condition	End of exposure		Maximum back surface exposure and temperature		Front surface temperature	
				Time, sec	Temperature, K	Time, sec	Temperature, K	Radiometer, K	Thermocouple, K
S-1	11	1	1	1849	427	2416	451	1520	(a)
		2		2382	460	2899	472	1470	
		3		2402	468	2900	481	1460	
		4		2568	460	2998	467	1500	
		5		2470	459	2970	467	1480	
		6		2546	552	3098	505	1450	
[b]S-2	9	1	2	696	461	978	512	1590	(a)
		2	3	702	461	1004	514	1570	
		3	4	679	466	1063	536	1610	
S-3	9	1	4	705	457	955	491	1610	(a)
		2	6	726	464	969	501	1650	
		3	7	678	461	922	503	1730	
		4	8	666	462	905	503	1750	
		5	9	649	467	890	516	1800	
		6	9	626	461	878	514	1830	
		7	9	624	464	872	517	1830	
		8	9	616	461	857	517	1840	
		9	9	611	461	849	518	1850	
S-4	9	1	2	753	460	917	469	1590	1440
		2	3	747	460	952	469	1580	1440
		3	4	687	461	889	473	1620	1490
		4	5	677	463	860	477	1620	1490
		5	7	635	466	837	482	1700	1530
S-5	9	1	5	603	464	787	484	1670	1520
		2	6	773	463	814	482	1670	1540
		3	7	576	461	795	485	1780	1600

[a]Surface thermocouple not installed.

[b]Test results for specimen S-2 are not reported after the third test cycle because the specimen was damaged during a tunnel malfunction.

TABLE 3.- TEST RESULTS - Continued

(b) Material MA

Specimen	Specimen size, cm	Test cycle	Test condition	End of exposure		Maximum back surface exposure and temperature		Front surface temperature	
				Time, sec	Temperature, K	Time, sec	Temperature, K	Radiometer, K	Thermocouple, K
MA II-1	13	1	1	648	427	968	504	----	(a)
		2		685	464	965	539	1410	
		3		703	466	988	538	1390	
MA III-1	9	1	2	277	464	438	531	1420	1320
		2	3	254	468	416	548	1490	1380
		3	4	228	463	366	562	1530	1410
		4	6	219	464	373	561	1600	(b)
		5	7	213	469	371	568	1670	(b)
		6	9	197	472	351	573	1750	(b)
MA III-2	9	1	2	265	465	418	527	1410	1310
		2	3	230	466	390	537	1490	(b)
		3	3	223	464	382	537	1510	(b)
MA III-3	9	1	2	271	463	413	518	1410	1310
		2		272	464	426	526	1480	1320
		3		265	466	418	529	1470	1320
		4		261	471	406	531	1510	1330
MA I-1	9	1	2	347	462	510	537	1480	1340
		2	3	335	462	494	542	1500	(b)
		3	4	315	465	475	553	1550	(b)
		4	6	295	463	454	557	1670	(b)
		5	7	288	466	452	560	1710	(b)
		6	9	272	463	436	561	1750	(b)
MA II-2	9	1	2	270	468	411	559	1500	(a)
		2	3	256	464	406	538	1520	
		3	4	231	467	375	572	1640	
		4	5	228	467	367	577	1670	
		5	6	226	468	372	577	1650	
		6	7	215	468	355	581	1720	
		7	8	213	478	339	579	1740	
		8	9	207	476	334	582	1770	

[a]Surface thermocouple not installed.

[b]Surface thermocouple installed but not operative.

TABLE 3.- TEST RESULTS – Concluded

(c) Material MB

Specimen	Specimen size, cm	Test cycle	Test condition	End of exposure		Maximum back surface exposure and temperature		Front surface temperature	
				Time, sec	Temperature, K	Time, sec	Temperature, K	Radiometer, K	Thermocouple, K
MB I-1	13	1	1	441	427	807	516	1830	(a)
MB I-2	13	1	1	501	427	868	523	----	(a)
		2	1	548	466	883	586	1780	
MB I-3	9	1	2	247	463	440	548	1790	(a)
		2	3	227	465	413	558	1850	
		3	4	191	466	371	568	1940	
		4	5	181	464	367	569	1990	
		5	6	181	462	365	564	1970	
		6	7	170	463	357	570	1980	
		7	8	175	461	360	573	1970	
MB II-1	9	1	2	200	462	328	571	1740	1410
		2	3	190	462	312	586	1820	1450
		3	4	173	466	299	600	1930	1510
		4	6	159	465	288	604	1980	(b)
		5	7	147	468	269	611	2050	(b)
MB II-2	9	1	2	203	464	326	571	1810	1410
		2	2	211	469	337	574	1790	1410
		3	3	197	469	321	583	1840	1450
		4	4	176	446	349	597	1950	1530

[a]Surface thermocouple not installed.

[b]Surface thermocouple installed but not operative.

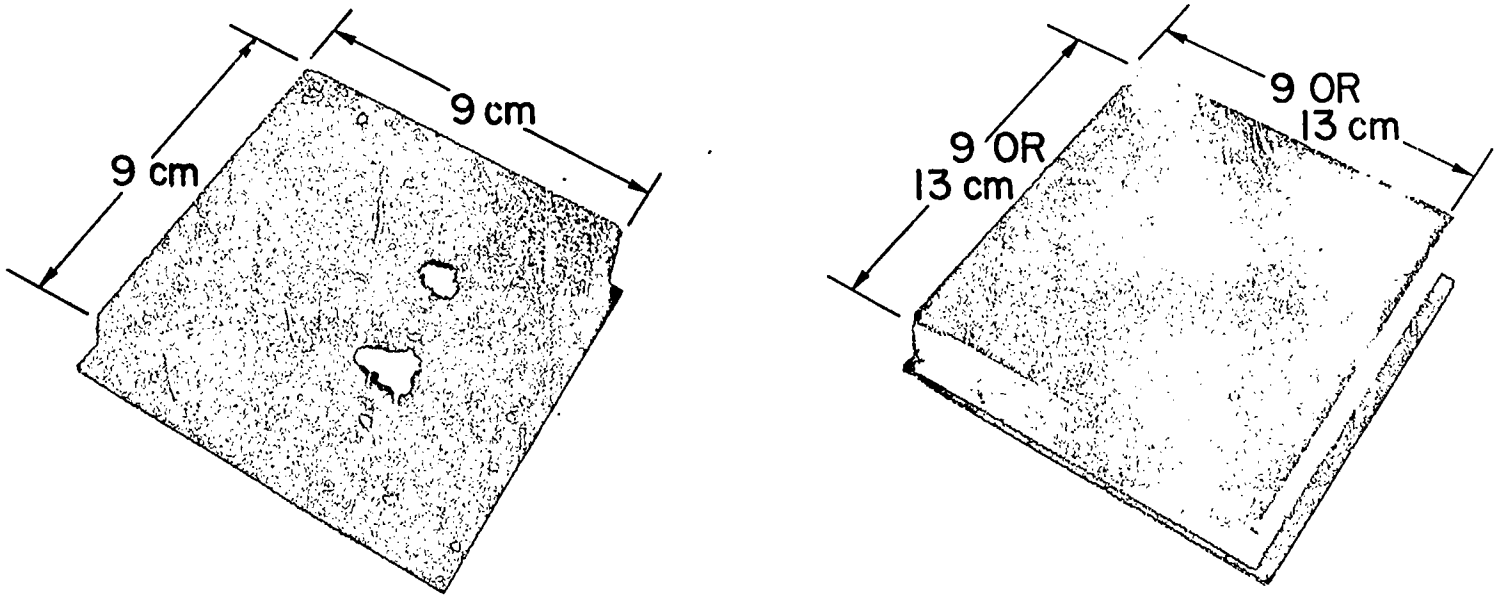

(a) Complete coating.

(b) Partial coating.

Figure 1.- Specimen configuration.

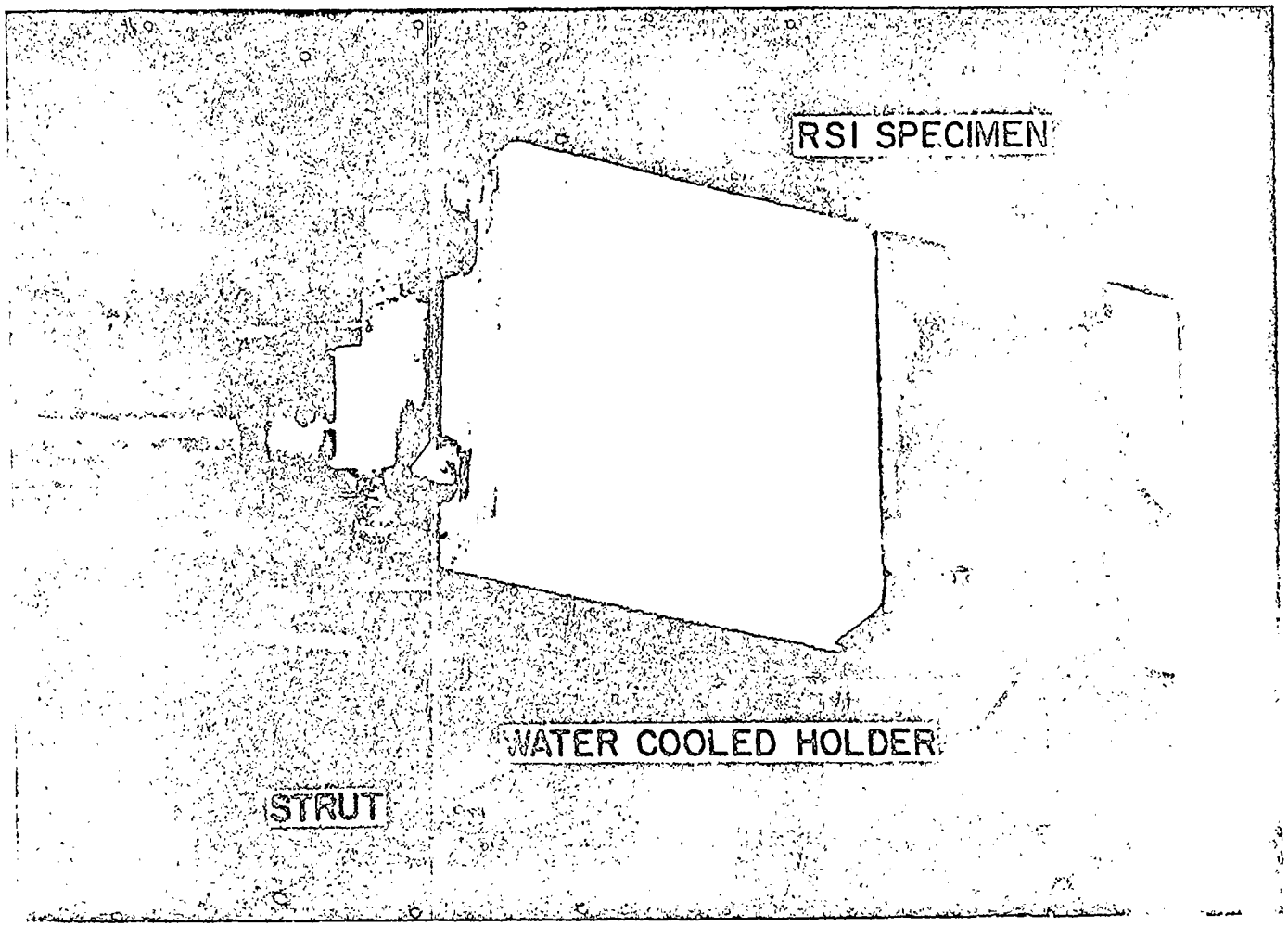

Figure 2.- Test configuration.

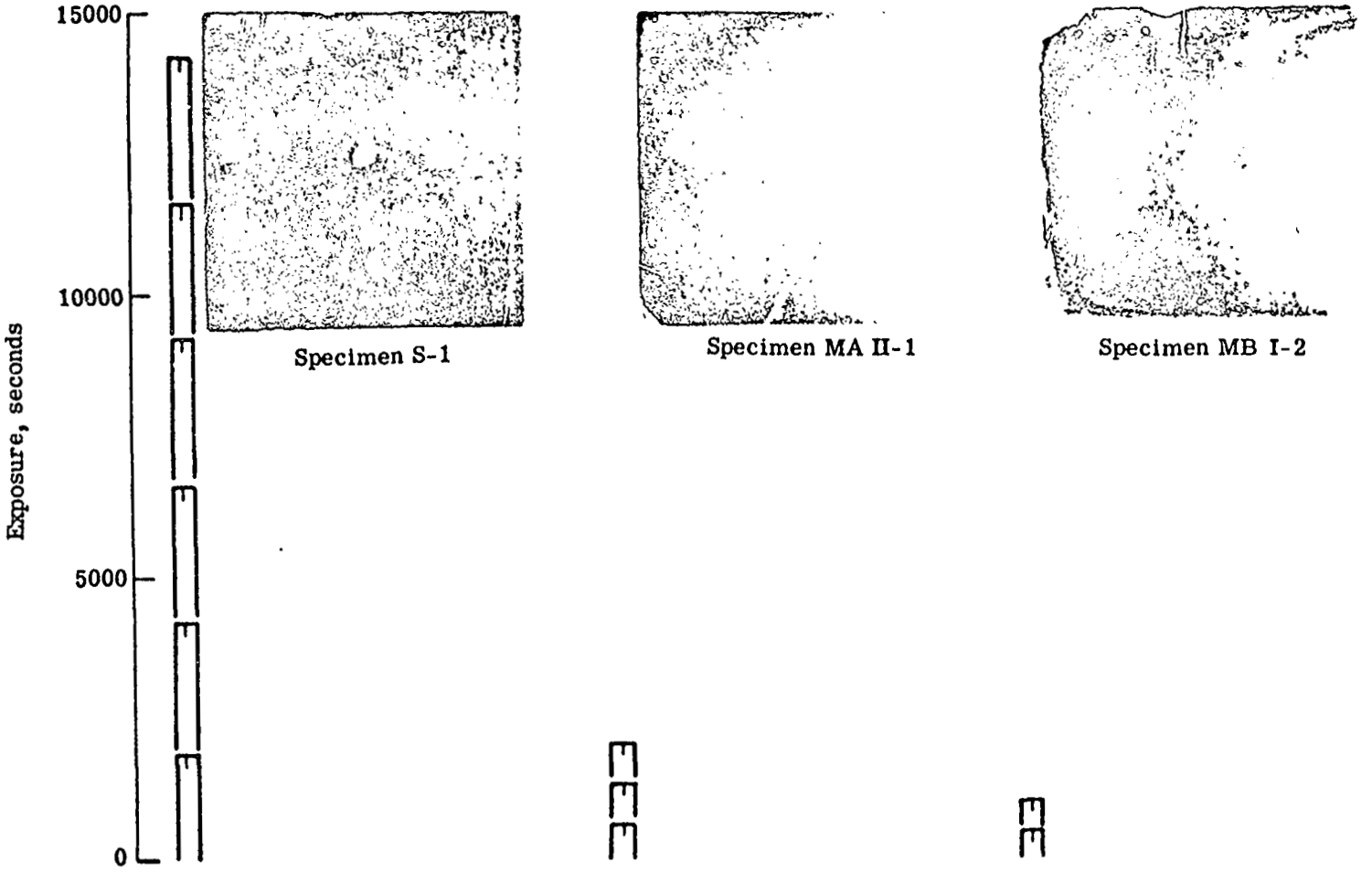

Figure 5.- Cumulative exposure time and specimen condition after testing at nominal shuttle entry conditions. Specimen size, 13 cm square; test stream direction from right to left.

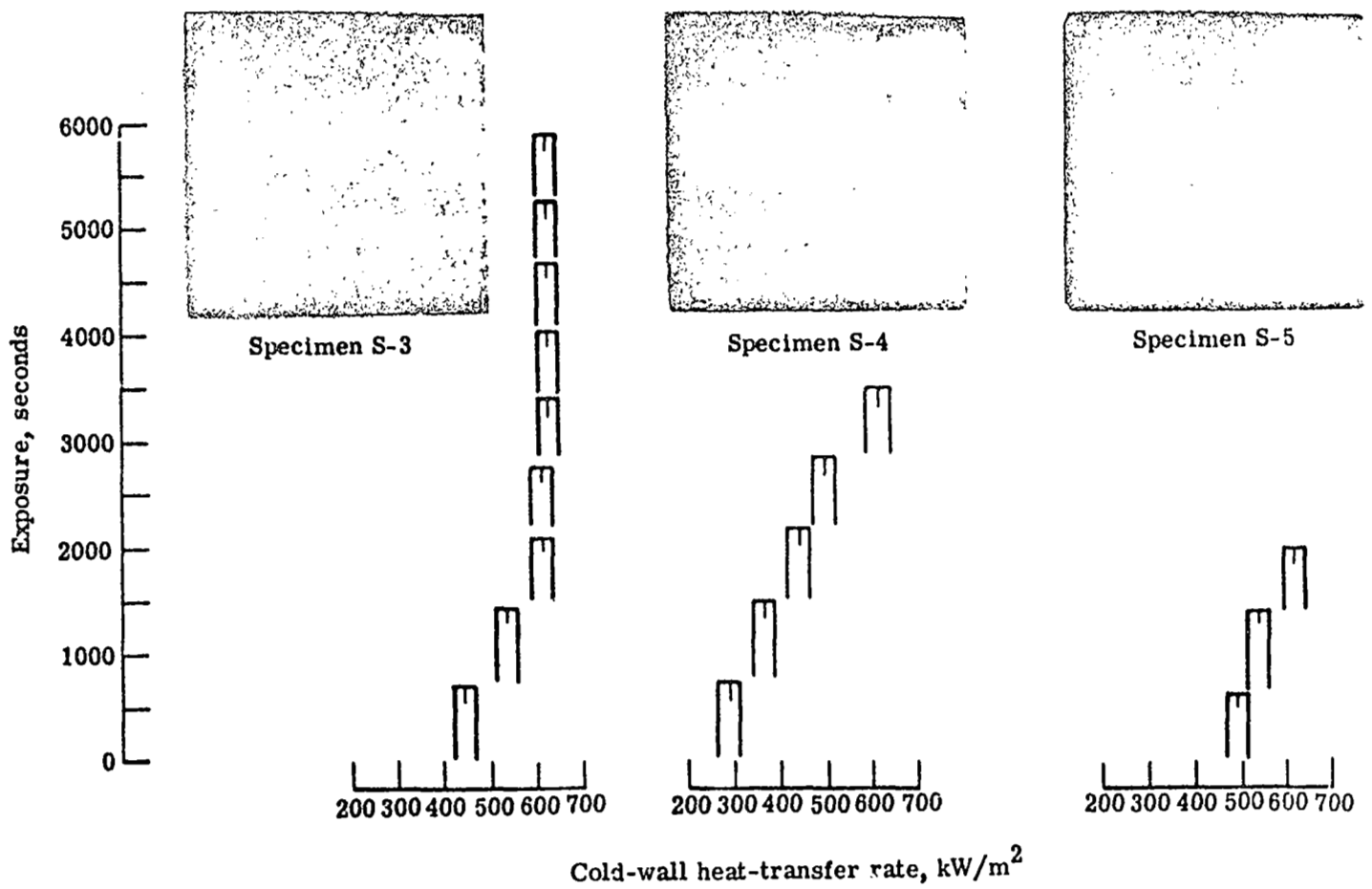

(a) Material S.

Figure 6.- Cumulative exposure time and specimen condition after testing at overdesign conditions. Specimen size, 9 cm square; test stream direction from right to left.

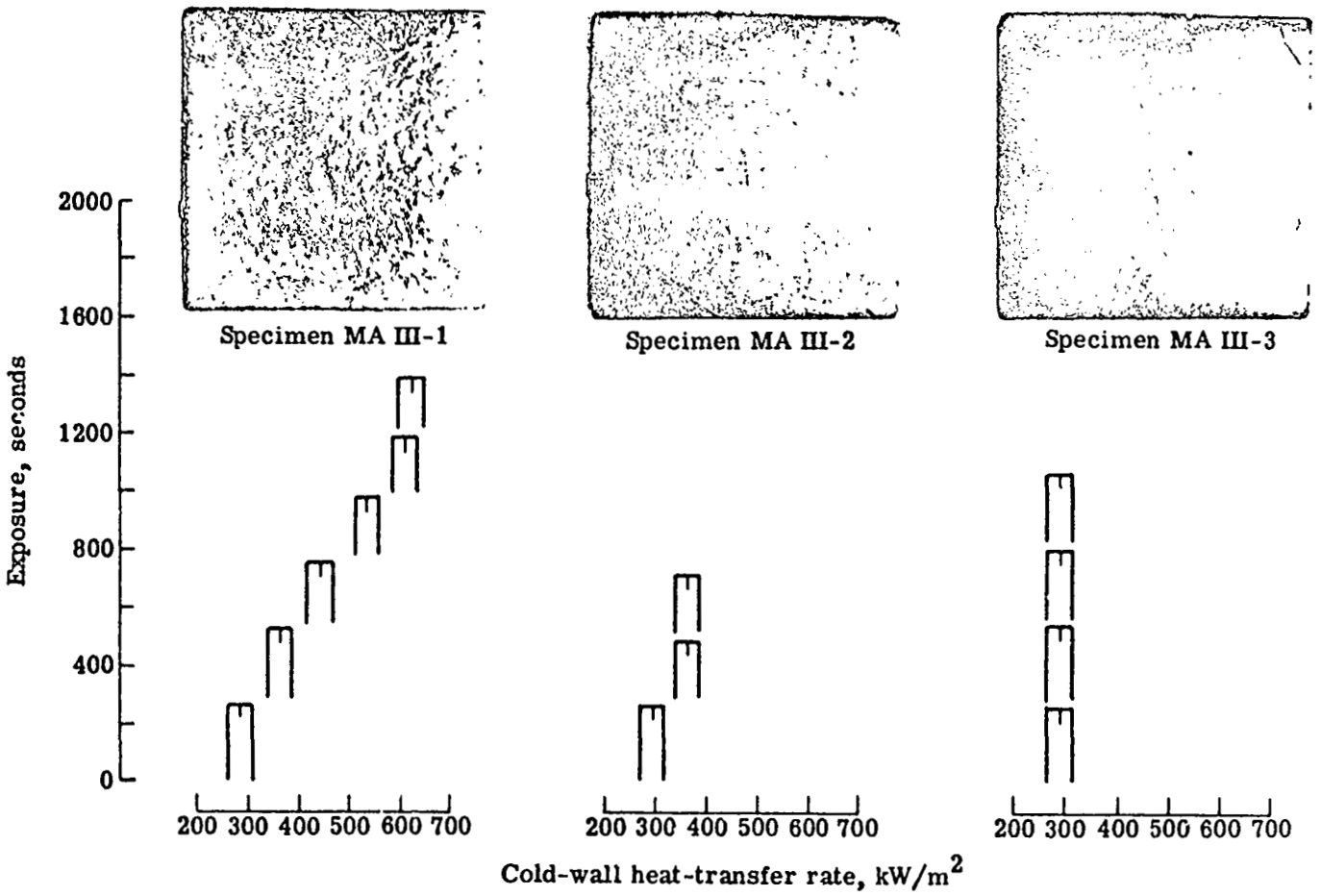

(b) Material MA III.

Figure 6.- Continued.

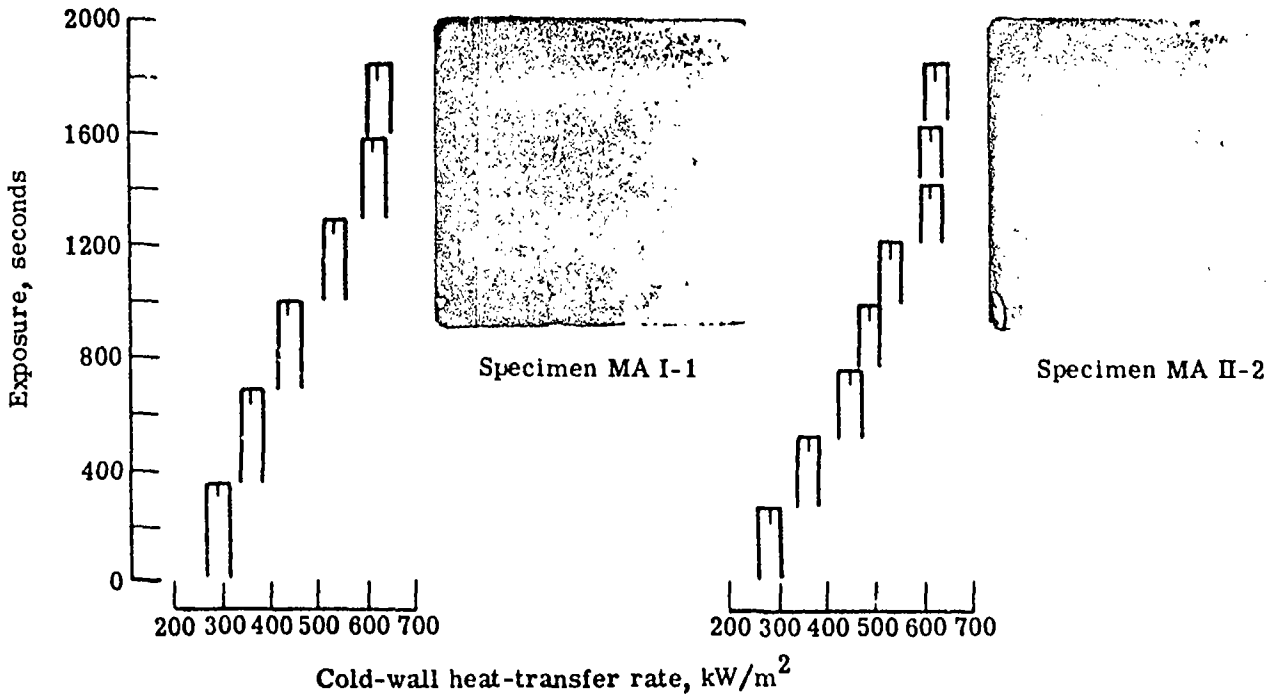

(c) Materials MA I and MA II.

Figure 6.- Continued.

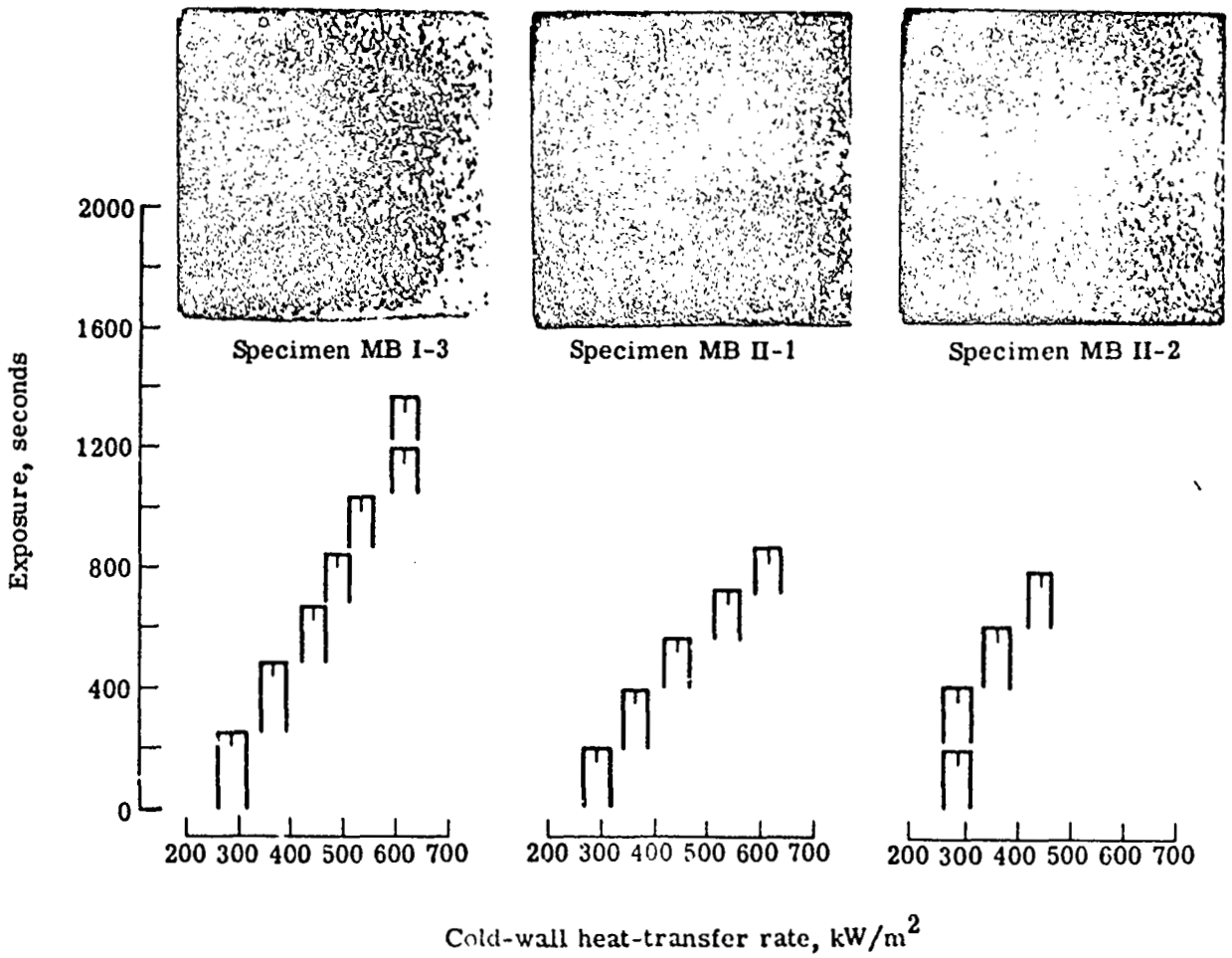

(d) Material MB.

Figure 6.- Concluded.

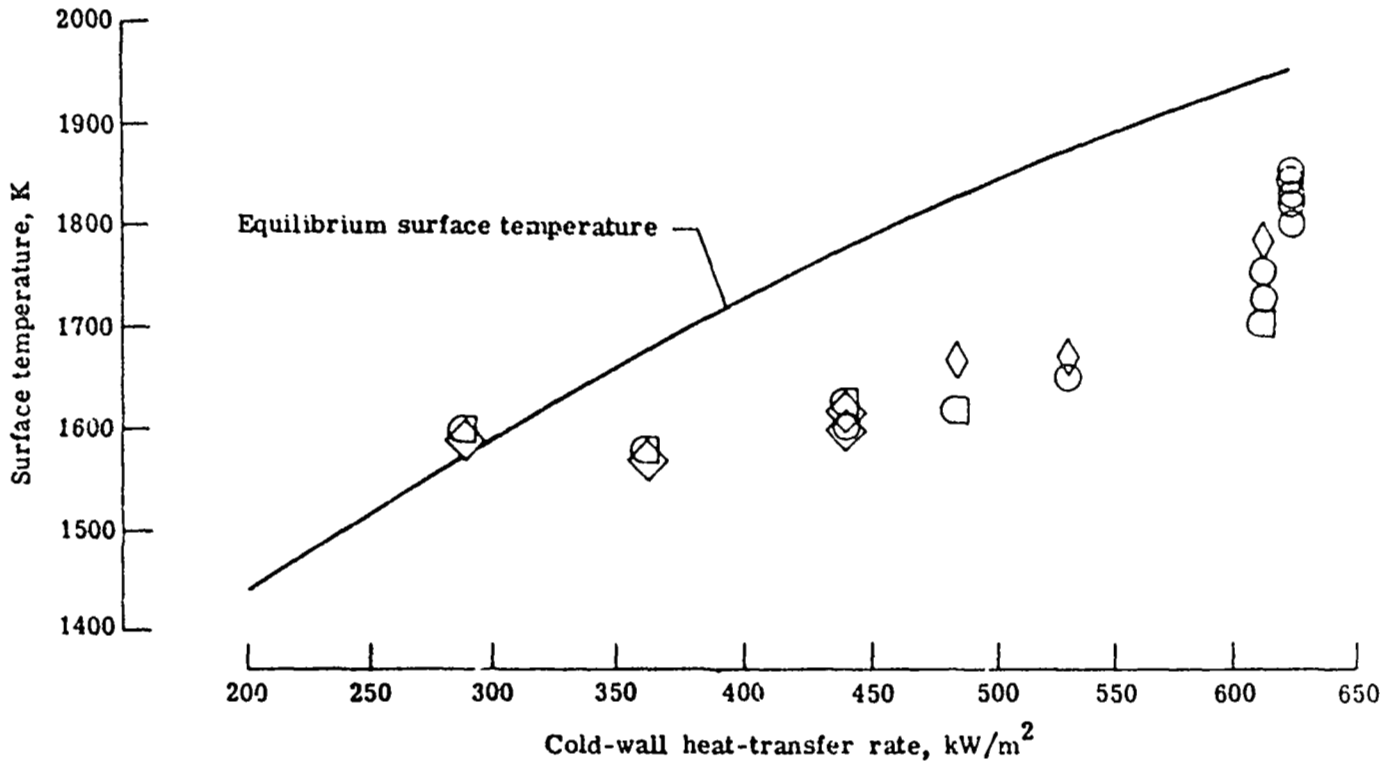

(a) Material S.

Figure 7.- RSI front surface temperature as a function of cold-wall heat-transfer rate.

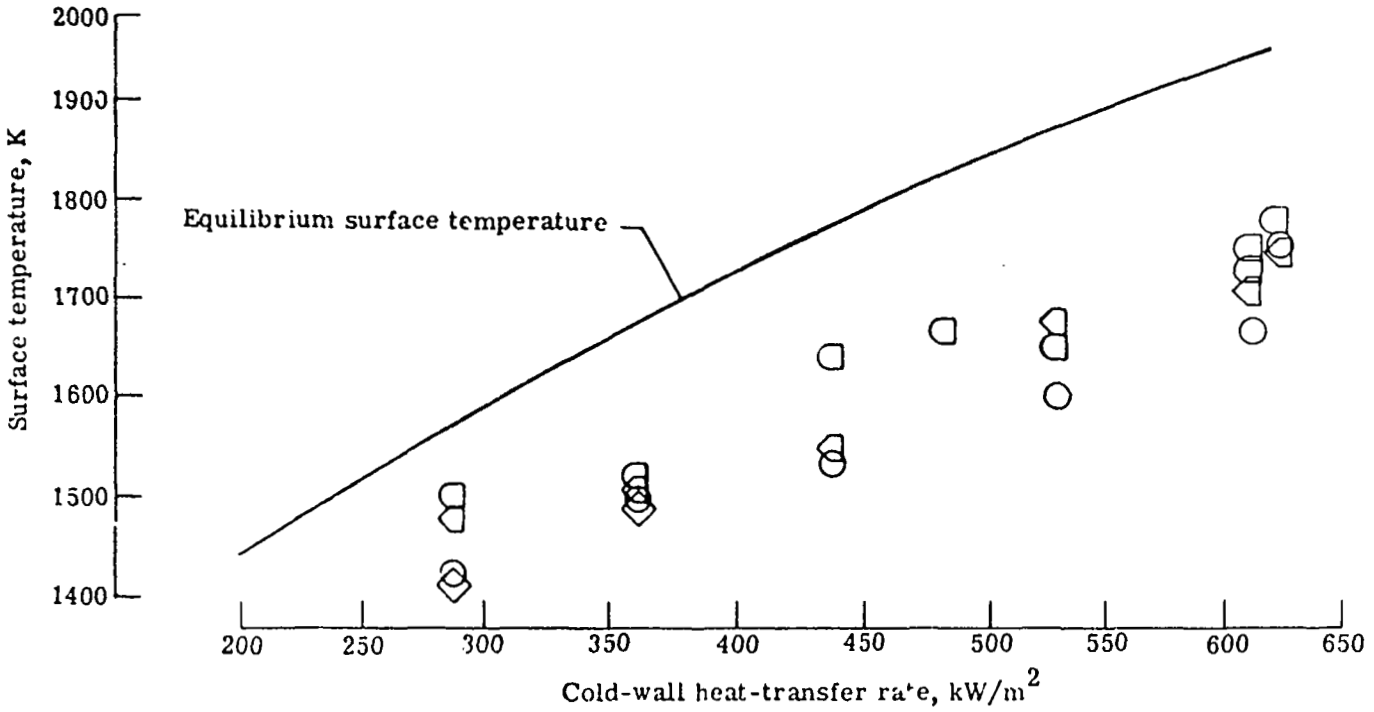

(b) Material MA.

Figure 7.- Continued.

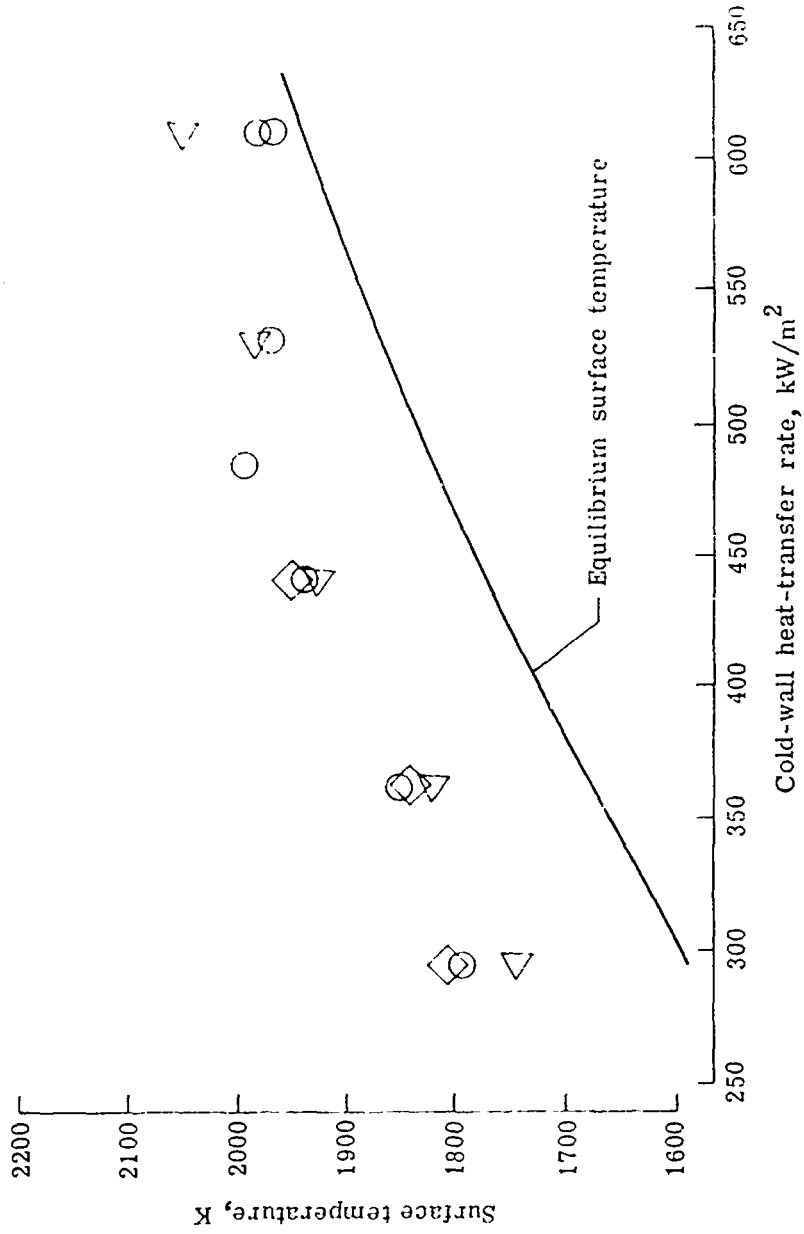

(c) Material MB.

Figure 7.- Concluded.

NASA Langley, 1973 — 18 L-8787

END

DATE

FILMED

NOV 28 1973